文章编号:2095-6134(2015)02-0145-10

Review Article

Plasma characteristics and dynamics in a high power pulsed magnetron sputtering discharge*

XIA Yuan†, GAO Fangyuan, LI Guang

(*Institute of Mechanics, Chinese Academy of Sciences, Beijing* 100190, *China*)

(Received 19 March 2014; Revised 25 July 2014)

Xia Y, Gao F Y, Li G. Plasma characteristics and dynamics in a high power pulsed magnetron sputtering discharge [J]. Journal of University of Chinese Academy of Sciences, 2015,32(2):145-154.

Abstract High power impulse magnetron sputtering (HIPIMS) is a promising technology that has drawn attention in both academia and industry in recent years. HIPIMS, also known as high power pulse magnetron sputtering, is a physical vapor deposition technique. The high power has been brought to extremely high discharge current density of several $A \cdot cm^{-2}$ and HIPIMS has been successfully developed to produce high plasma densities of the order of 10^{19} m^{-3}. The plasma properties in sputtering process have shown the great advantages, which make it possible to control the deposition process and optimize the performance of films. In this paper, we show the I-V characteristics of discharge and the design of power supply, as well as the ionization rate of sputtered atoms. Furthermore, the spatial and the temporal evolution of plasma, the non-normal transport of ionized species, and the deposition rate are reviewed.

Key words HIPIMS; HPPMS; plasma dynamics; discharge characteristic; high ionization rate

CLC Number: TB43 **Document code**: A **doi**: 10.7523/j.issn.2095-6134.2015.02.001

高功率脉冲磁控溅射等离子体特性与动力学研究进展

夏 原, 高方圆, 李 光

(中国科学院力学研究所, 北京 100190)

摘 要 高功率脉冲磁控溅射(HIPIMS)作为一项极具发展前途的物理气相沉积新技术,近年来引起学术界和工业界的广泛关注. HIPIMS 技术(也被称为 HPPMS)可以提供足够的放电功率来获得极高的电流密度,数值达到几个 $A \cdot cm^{-2}$;同时,可以得到 10^{19} m^{-3} 量级的高密度等离子体. 溅射过程中独特的等离子体特性表明了该技术的突出优势,因此可实现沉积过程的控制和薄膜性能的优化. 文中对 HIPIMS 技术的 IV 放电特征,电源设计,以及溅射原子离化率进行深入分析. 同时,回顾讨论等离子体时间空间演变规律,离化基团输运,薄膜沉积速率等问题的

* Supported by the Research Equipment Development Project of Chinese Academy of Sciences (YZ201135)

† Corresponding author, E-mail: xia@imech.ac.cn

研究进展.
关键词 HIPIMS；HPPMS；等离子体动力学；放电特性；高离化率

Magnetron sputtering as a well-established physical vapor deposition (PVD) technique has been used to deposit different coatings for a wide range of applications. Because of the ability to be easily controlled by electric and magnetic fields, the charged particles such as ions are advantageous for facilitating plasma-ion processing. Therefore, the efficient production of charged particles is indispensable for current PVD techniques. High power impulse magnetron sputtering (HIPIMS) is a promising technique for ion assisted film growth and surface engineering, by which nearly full ionization of the sputtered Ti atoms has been obtained[1]. The method was introduced by Kouznetsov et al.[2], and has drawn attention in both academia and industry in recent years[3-4].

In HIPIMS, the high power leads to peak electron densities exceeding 10^{19} m^{-3} in the positions close to targets, which are three times higher than those achieved by conventional sputtering techniques[5-6]. The high density of electron increases the ionization impact probability between sputtered atom and high energy electron, therefore high ionization sputtering material particles are gained. Through the control of electric and magnetic fields, the charged particles can obtain higher ion energy. It is precisely the reason that HIPIMS has been successfully developed to obtain high-quality films with high adhesion, high density, and good corrosion resistance and wear resistance. This technique has been demonstrated to be useful for substrate cleaning, high-aspect-ratio filling application and improvement of microstructure of thin films[1,2,7-10].

Many studies[11-14] indicate that plasma environment has a significant impact on structure and properties of the films in deposition process. Therefore, to better control the film growth process, to find the optimal experimental conditions, and to obtain high quality thin films, further study of the plasma characteristics and transport dynamics is necessary. Great attention has been paid to the unique plasma properties in sputtering process with the developement of HIPIMS. Extensive investigations have shown the outstanding advantages of HIPIMS compared with other magnetron sputtering techniques, from the initial electron density[5,15] to the recent distribution of ion energy[16-18]. In the following sections, the typical characteristics and dynamics of plasma in HIPIMS will be discussed to clarify its illustrious excellences in industrial applications.

1 *I-V* characteristics of gas discharge in HIPIMS

As early as in 1903, Townsend explained the mechanism of gas discharge using the concept of gas ionization, namely the Townsend theory. The discharge characteristic curve of low pressure gas is shown in Fig. 1, and the curre is mainly divided into normal glow discharge, abnormal glow discharge, and arc discharge pant. Studies showed that the *I-V* characteristics of conventional DC magnetron sputtering (dcMS) are mainly located in the early stage of abnormal glow discharge, while those of cathodic arc (CA) are located in the stage of arc discharge. In fact, the exploration of HIPIMS has filled the gap between the dcMS and the CA. The *I-V* characteristic curves of HIPIMS meet the back-end of abnormal glow discharge region, and therefore are more difficult to control as the instability.

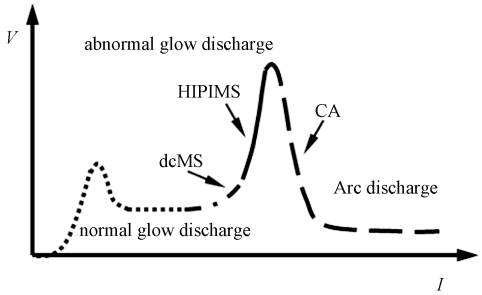

Fig. 1 Discharge characteristic curve of low pressure gas

In DC magnetron sputtering, the target current I_d and the target voltage V_d follow a certain functional relation: $I_d = K_d V_d^{\,n}$[19], where K_d is a constant. The exponent n is typically within the range of 5 ~ 15, which mainly depends on the target material type, magnetic field, and other experimental parameters. In HIPIMS, there is also a similar function between the peak target current density and the target voltage. Figure 2 shows the target voltage versus the peak target current density for a conventional DC magnetron sputtering discharge and a HIPIMS discharge, respectively[20]. For the conventional DC magnetron sputtering, the exponent n is approximately 8. The HIPIMS discharge exhibits two slopes depending on the target current. For the low current density region, the exponent n is about 7, indicating the conventional magnetron sputtering discharge mode. At higher current density, the exponent n is suddenly reduced to 1, which is well consistent with the Townsend curve. Alami et al.[21] have carried out the similar research about the sudden change in discharge pattern. This sudden increase in the resistance of discharge has been considered to be caused by a sharp reduced capture of secondary electrons[20].

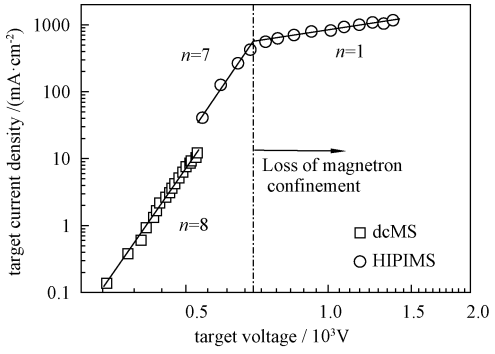

Fig. 2　Target voltage versus peak target current density for a magnetron in dcMS and HIPIMS modes, respectively[20]

2　Plasma characteristics in HIPIMS

2.1　High discharge current density

For conventional magnetron sputtering, the maximum power is limited because of the thermal load on the target provided by the bombardment of positive ions. To avoid this limitation, high-power pulsed magnetron sputtering introduced a method by making a lower duty cycle (on-time divided by the cycle-time), while a corresponding increase in power during the on-time. This not only has resolved the thermal load problem, but also brought the peak discharge current density to the order of several $A \cdot cm^{-2}$[1,2,20]. HIPIMS power is mainly based on single or multiple LC circuit networks[22-24]. The voltage and current waveform is determined not only by the power supply but also by the load, such as magnetron sputtering device, magnetic field structure, target material, gas type, and pressure of the vacuum chamber[5,25-29].

Figure 3 shows how the pulse shapes depend on the argon pressure[5]. It can be seen that the plasma ignition point has a close relationship with the gas pressure. With the increase of gas pressure the pulse duration decreased, and the plasma ionization could be achieved instantly without time delay in the case of low pressure. To solve the problem of time delay, the plasma is pre-ionized by a DC power supply in some of the high power pulse systems[8,30-32].

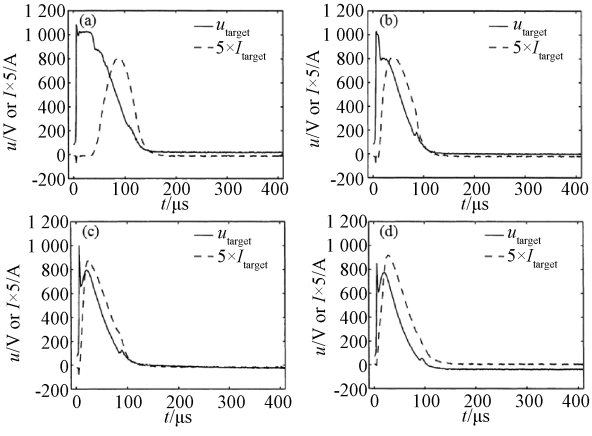

Fig. 3　Target current and voltage waveform produced by the HIPIMS power supply at working pressures of (a)0.06 Pa, (b)0.26 Pa, (c)1.33 Pa, and (d)2.66 Pa[5]

2.2　High ionization rate

Compared with the conventional magnetron sputtering methods, in which the ions available are mainly the ions of the inert sputtering gas, a high degree of ionization of the sputtered atoms is a

significant feature for HIPIMS. Optical emission spectroscopy (OES) studies have confirmed an enhanced proportion of ions of both residual gas and sputtered species in the HIPIMS discharge[7, 20, 32-34]. Figure 4 shows the typical OES spectra from HIPIMS and conventional magnetron sputtering discharges of Cr in Ar at the same average power[7]. Strong emission from Cr ions is observed in the HIPIMS plasma, both singly and doubly ionized, while the ratio of Cr ion to neutral spectral line is negligible in the conventional magnetron sputtering. As a result, the ionization rate increased significantly, and the ionized flux fraction for Cr had been estimated to be roughly 30% by the weight gain method.

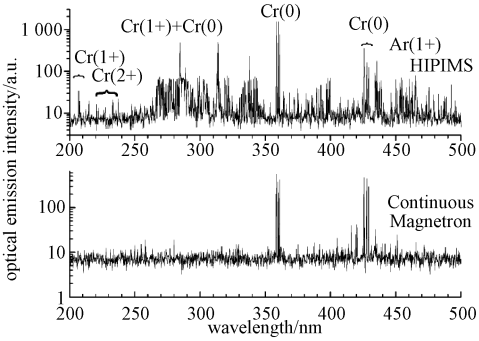

Fig. 4 Typical OES spectra for the plasma composition in HIPIMS and conventional magnetron sputtering of Cr in Ar atmosphere at the same average power[7]

Konstantinidis et al.[33] showed that the ionization rate is higher than 50% for a Ti target and increases with increasing applied power and pulse length. Bohlmark et al.[34] also observed the ion contribution of the sputtered Ti increases with increasing applied pulse energy and reaches values higher than 90%. The ion-to-neutral ratios as a function of the peak target current of the sputtered Cr are shown in Fig. 5[20]. The diagnostic results indicate an increased ion-to-neutral ratios of Cr^{2+}/Cr^{0} and Cr^{1+}/Cr^{0} with target current. It can be also concluded that the degree of ionization is very high for Cr. Bohlmark et al.[32] showed that the ion flux contained more metal ions (Ti^{1+} 50%, Ti^{2+} 24%) than inert gas ions (Ar^{1+} 23%, Ar^{2+} 3%) during the intense moment of the discharge. The peak Ti^{1+}/Ar^{1+} ratio is over two. Therefore, the HIPIMS discharge is highly metallic containing.

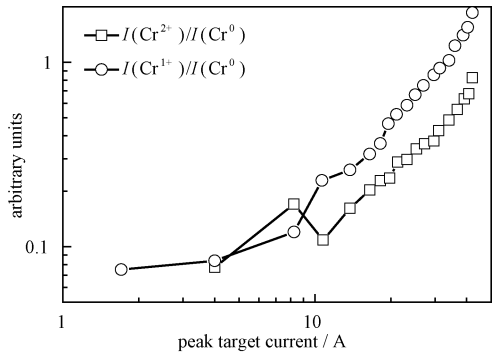

Fig. 5 Ion-to-neutral ratio as a function of the peak target current for Cr from optical emission line intensities[20]

2.3 High ion energy distribution

It is well known that the trajectory can be changed in an $E \times B$ drift loop only for the charged particles. The high degree of ionization creates new opportunities, since the ions can be controlled by using electric or magnetic fields and obtain higher ion energy. The ion energy distribution function (IEDF) for an HIPIMS and a dcMS discharges are shown in Fig. 6[32]. There are distinct differences in the energy distribution observed for the two techniques. For HIPIMS, the ion energy distribution is broader, extending to a more intense high-energy tail, 100 eV. The energy of about 50% of the Ti ions is higher than 20 eV. Similar results have been observed by Erkens et al.[35] and Lin et al.[36].

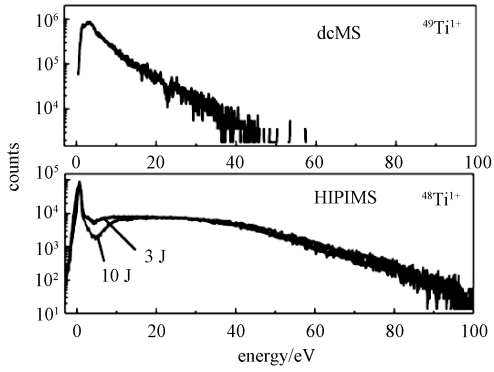

Fig. 6 Ion energy distributions for Ti^{1+} ions measured in dcMS and HIPIMS discharges[32]

Due to the large fraction of energetic ions produced by HIPIMS, the technique provides high-quality films with excellent adhesion, high density, and smooth surfaces. The energetic ions can serve as

effective adhesion promoters for momentum transfer and film densification during film growth. Figure 7 shows the chemical composition profile of the CrN coating in which the substrate was pretreated by HIPIMS with the negative voltage of 1 200 V[7]. A transition region with a width of approximately 40 nm is confirmed, while Cr increases and Fe decreases. It can be considered that Cr is implanted in the stainless steel substrates. An incorporation of 4 at. % of Ar is characterized at the interface, which is a result of the high energy gas/metal ion etching[37]. This process was shown to enhance the adhesion with values of LC up to 85 N[7]. The microstructure of interfaces pretreated by HIPIMS of Cr is shown in Fig. 8[38]. The interface is clean and dense, which appears to be a clear boundary owing to the intensive bombardment by high fractions of metal ions. Therefore, the presence of high-energy

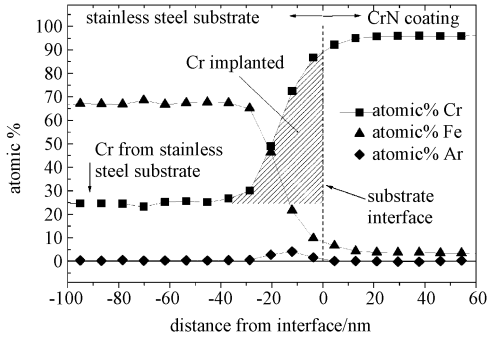

Fig. 7　STEM-EDS analysis of the chemical composition at the coating-substrate interface after pretreatment and CrN coating deposition by HIPIMS[7]

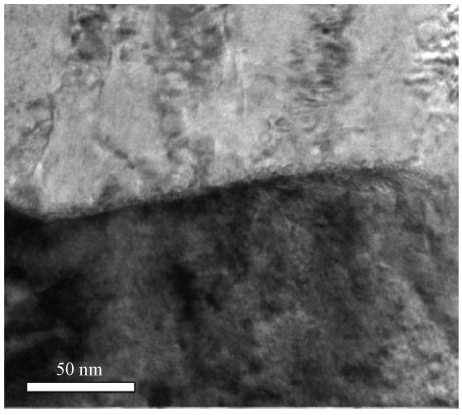

Fig. 8　Cross sectional views of the interface between the CrN base layer and the stainless steel substrate pretreated by HIPIMS with U_{bias} = −1 000 V[38]

ions is significant for the improvements in coating adhesion, structure, and properties.

3　Plasma dynamics in HIPIMS

In the process of film growth, the plasma conditions across the chamber have a significant impact on the performance of films. Better mapping of the plasma dynamics is therefore necessary to fix process parameters and optimize preparations for films in an HIPIMS system. The following text will be divided into three stages, occurrence, transport, and deposition, to describe the research results on plasma dynamics in HIPIMS.

3.1　Occurrence

The discharge characteristics of HIPIMS have been studied by Anders et al.[26]. The discharge consists of two phases. The first phase can be ascribed to argon ions and secondary electrons generated by them, and the immediately followed second stage depends on the sustained self-sputtering which can provide high power. The self-sputter-dominated phase not only strongly depends on the material, but also the correlation with the secondary electrons. The yield of secondary electrons strongly depends on the potential energy of the primary ions, and the generation of charged metal ions is critical for the maintenance of the self-sputter dominated phase. Self-sputter yields for various target materials as a function of primary ion kinetic energy is shown in Fig. 9[26]. It can be seen that carbon has a very small sputter yield and thus it can not go in the self-sputter dominated mode. Other materials all have the self-sputter dominated phase in their own pronounced manner.

The ionization mechanism in an HIPIMS discharge has been reported[39]. The results show that a large number of electrons are trapped in the magnetic field near the targets during the pulse-on period and the most effective process in creating metal ions is the electron impact ionization. After the pulse is off, charge exchange becomes the dominant process in ionization of metal atoms.

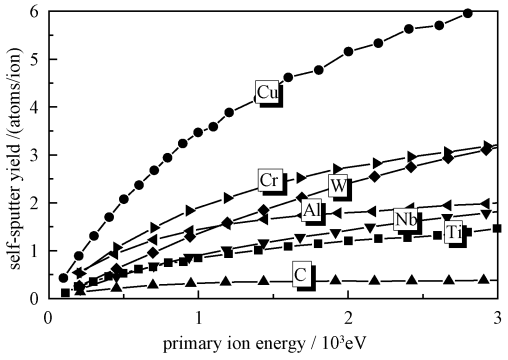

Fig. 9 SRIM-calculated self-sputter yields as functions of primary ion kinetic energy for various target materials[26]

3.2 Transport

The spatial and temporal variation in the plasma parameters such as electron density, average electron energy, plasma potential, and electron energy distribution function (EEDF) can be calculated from *I-V* curves obtained by Langmuir probes[2,5,15,20]. Gudmundsson et al.[5] have observed the time-dependent electron density for different pressures and distances away from the target cathode. The peak electron density is in the range of $(2-8)\times10^{18}$ m^{-3} and decreases with the decreasing inert gas pressure or the increasing distance. The spatial and temporal evolution of the electron density in a plane perpendicular to the surface of the magnetron has been explored by Bohlmark et al.[40]. A high-density doughnut shaped plasma forms above the race track in the early stage of the discharge. It demonstrates how the high density plasma expands away from the target surface. The trajectories of the peak intensity of the expanding plasma at three different Ar pressures are shown in Fig. 10[5]. This peak travels away from the target with a fixed velocity, which decreases with increasing operating pressure. A best fit through the data gives the traveling velocity of the electron density peak of 4.0×10^5 cm/s at 0.06 Pa, 1.8×10^5 cm/s at 0.26 Pa, and 0.8×10^5 cm/s at 1.33 Pa.

The evolution of the electron energy distribution function (EEDF) with time from initiating the pulse has been reported[15,41]. According to the measured *I-V* characteristics of a Langmuir probe, the EEDF is determined using the Druyvesteyn formula[42-43]. Initially, the distribution can be described by a single peak indicating a Druyvesteyn like. Towards the end of the pulse, two energy groups of electrons are present. With the disappearance of the high-energy electron group, the electron energy distribution appears to be Maxwellian like. Eventually, the plasma becomes more Druyvesteyn like with lower electron density and higher average electron energy.

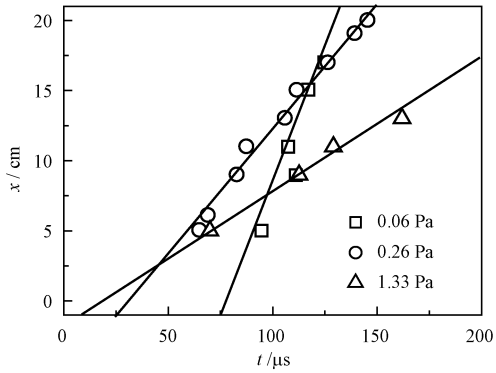

Fig. 10 Trajectory of the peak intensity of the expanding plasma at different Ar pressures[5]

The temporal behavior of the plasma density was influenced by the process conditions such as sputtering gas, chamber dimension, distance to target, and applied power[25]. The time evolution has also been measured for the ion species in the plasma[44-45]. Figure 11 shows the integrals of the ion energy distribution function, as a measure of the number of ions entering the mass spectrometer[46].

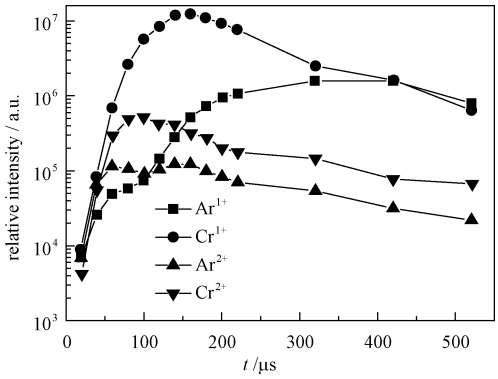

Fig. 11 Integrals of the IEDF in HIPIMS plasma discharge with Cr target[46]

Since the start of the pulse, the Cr^{1+} flux dominates the value until 420 μs when more Ar^{1+} ions are detected. The peak of the Cr^{1+} ion flux has been ten times the peak of the Ar^{1+} ions. The Ar^{2+} ion flux seems to have two extrema, the first one coming with metal ions and the second one coming with the Ar^{1+} flux. The first wave could be due to the energy transferred from sputtering particles to nearby gas particles, while the second wave could originate from the particles near the target region.

Measured with the thermal probe facing the magnetron surface, the energy flux distribution in an HIPIMS plasma of approximate 500 W average power is presented in Fig. 12[47], while the previous investigations on energy flux have been mainly focused on the axial flux[48]. It is indicated that the heat flux increases towards the surface of the magnetron and peaks in the region between the race track ($\rho = 4.5$ cm) and the rim of the magnetron. Compared with the centre at $\rho = 0$ cm, the energy flux is as twice large as at $\rho = 8$ cm in the near-cathode region ($z = 4$ cm). The energy flux profile shows more homogeneously distributed away from the cathode surface, and the radial variation of the energy flux is rather small at $z > 10$ cm.

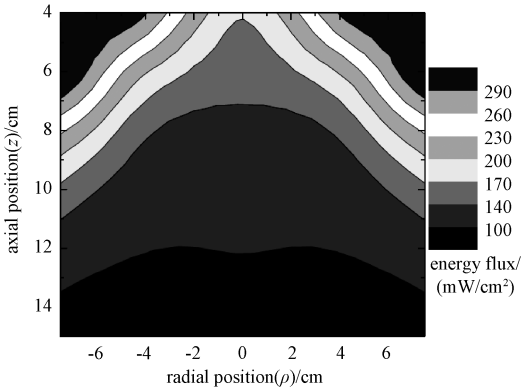

Fig. 12　Energy flux distribution at the radial (ρ) and axial (z) by HIPIMS at average power of 500 W[47]

3.3　Deposition

Compared to the atoms, the high-energy ions are provided with better diffraction gain in electromagnetic field, and thus the films prepared by HIPIMS greatly improve the uniformity and flatness[49-50]. The technology is widely used for high-aspect-ratio filling and high-quality films preparation. However, in the HIPIMS discharge, the deposition rate is found to be generally lower than in a conventional dcMS discharge for an equivalent amount of power[51-55]. Konstantinidis et al.[54] found the effect of the pulse on/off time configuration on the deposition rate of films grown by HIPIMS, and as the pulse length decreases from 20 μs to 5 μs for the same average power, the deposition rate increases from 20% to 70% of dcMS values. Figure 13 shows the obtained deposition rates for dcMS and HIPIMS by using an equal average power with different inclination angles of the substrates[55]. When samples grown facing the target surface ($\theta = 0°$), the deposition rate for HIPIMS is approximately 40% in DC sputtering. However, it is seen that the deposition rate of dcMS suffers from a significantly larger decrease than HIPIMS for substrates placed at a large angle ($\theta > 90°$). For HIPIMS films grown at the inclination angle of 90°, the deposition rate dropped to about 42% of the value measured at the inclination angle of 0°, while the corresponding values for dcMS reduced to 17% as demonstrated. The results further reflect that the plasma in HIPIMS possesses better diffraction.

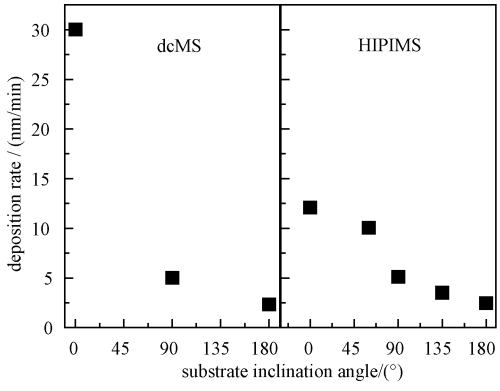

Fig. 13　Normalized deposition rates measured for films grown by dcMS and HIPIMS at different inclination angles[55]

The decreased deposition rate in HIPIMS has been explained mainly by the fact that the ions can be attracted back toward the target and captured by the cathode potential[56]. The reduction is expected

to occur especially for metals with a low self-sputtering yield. The deposition efficiency for HIPIMS compared with a dcMS discharge plotted as a function of the metals self-sputtering yield divided by its Ar-sputter yield is developed by Christie[53]. Some other possible explanations for the reduction in deposition rate in HIPIMS are due to the low conductivity or magnetic confinement in the target-to-substrate region[54,57]. Recent results show that the deposition rate can be optimized by placing an rf-driven inductively coupled discharge[58] or applying a magnetic coil[59] between the target and the substrate. Therefore, the problem of a lower deposition rate can be solved through a number of methods.

4 Expectation

The studies on plasma dynamics in HIPIMS process have been reviewed. The main emphasis in this work was placed on the newly developed PVD technique which provides high power densities, high ionization fraction, and high ion energy distribution. With the outstanding advantages, the technique already plays an important role in various coating applications, such as conformal growth of films on non-flat substrates, substrate pre-treatment for improved adhesion, and preparation of high-performance thin films.

So far, several groups not only studied the physical properties of plasma, but also showed solicitude for the relationship between experimental parameters and film structures[60-62]. However, the researches lack the discussion about their intermediate "plasma", which is crucial for increasing film production in the stability and repeatability. Therefore, the development trend in future will be, by studying and interpreting the secrets of "plasma", to achieve the relationships among experimental parameters, plasma, and film structures, and to provide the basis for the realization of industrial production.

References

[1] Bohlmark J, Alami J, Christou C, et al. Ionization of sputtered metals in high power pulsed magnetron sputtering [J]. J Vac Sci Technol, A, Vac Surf Films, 2005, 23(1): 18-23.

[2] Kouznetsov V, Macúk K, Schneider J M, et al. A novel pulsed magnetron sputter technique utilizing very high target power densities[J]. Surf Coat Technol, 1999, 122(2/3): 290-293.

[3] Sarakinos K, Alami J, Konstantinidis S. High power pulsed magnetron sputtering: a review on scientific and engineering state of the art [J]. Surf Coat Technol, 2010, 204(11): 1 661-1 684.

[4] Gudmundsson J T, Brenning N, Lundin D, et al. High power impulse magnetron sputtering discharge [J]. J Vac Sci Technol A, 2012, 30(3): 030 801-18.

[5] Gudmundsson J T, Alami J, Helmersson U. Spatial and temporal behavior of the plasma parameters in a pulsed magnetron discharge[J]. Surf Coat Technol, 2002, 161(2/3): 249-256.

[6] Bohlmark J, Gudmundsson J T, Alami J, et al. Spatial electron density distribution in a high-power pulsed magnetron discharge [J]. IEEE Trans Plasma Sci, 2005, 33(2): 346-347.

[7] Ehiasarian A P, Münz W D, Hultman L, et al. High power pulsed magnetron sputtered CrNx films [J]. Surf Coat Technol, 2003, 163-164: 267-272.

[8] Vůsina P, Měsko M, Ganciu M, et al. Reduction of transient regime in fast preionized high-power pulsed-magnetron discharge[J]. Europhys Lett, 2005, 72(3): 390-395.

[9] Alami J, Eklund P, Emmerlich J, et al. High-power impulse magnetron sputtering of Ti-Si-C thin films from a Ti_3SiC_2 compound target [J]. Thin Solid Films, 2006, 515(4): 1 731-1 736.

[10] Reinhard C, Ehiasarian A P, Hovsepian P Eh. CrN/NbN superlattice structured coatings with enhanced corrosion resistance achieved by high power impulse magnetron sputtering interface pre-treatment [J]. Thin Solid Films, 2007, 515(7/8): 3 685-3 692.

[11] Anders A, Ni P, Rauch A. Drifting localization of ionization runaway: Unraveling the nature of anomalous transport in high power impulse magnetron sputtering[J]. J Appl Phys, 2012, 111(5): 053 304-13.

[12] Anders A. Self-organization and self-limitation in high power impulse magnetron sputtering [J]. Appl Phys Lett, 2012, 100(22): 224 104-5.

[13] Ehiasarian A P, Hecimovic A, Arcos T de los, et al. High power impulse magnetron sputtering discharges: instabilities

and plasma self-organization[J]. Appl Phys Lett, 2012, 100 (11): 114 101-4.

[14] Kozyrev A V, Sochugov N S, Oskomov K V, et al. Optical studies of plasma inhomogeneities in a high-current pulsed magnetron discharge[J]. Plasma Phys Rep, 2011, 37(7): 621-627.

[15] Gudmundsson J T, Alami J, Helmersson U. Evolution of the electron energy distribution and plasma parameters in a pulsed magnetron discharge[J]. Appl Phys Lett, 2001, 78 (22): 3 427-3 429.

[16] Lin J, Moore J J, Sproul W D, et al. Ion energy and mass distributions of the plasma during modulated pulse power magnetron sputtering[J]. Surf Coat Technol, 2009, 203 (24): 3 676-3 685.

[17] Oks E M, Anders A. Boron-rich plasma by high power impulse magnetron sputtering of lanthanum hexaboride[J]. J Appl Phys, 2012, 112(8): 086 103-3.

[18] Bowes M, Poolcharuansin P, Bradley J W. Negative ion energy distributions in reactive HiPIMS[J]. J Phys D: Applm Phys, 2013, 46(4): 045 204-9.

[19] Rossnagel S M, Kaufman H R. Current voltage relations in magnetrons[J]. J Vac Sci Technol A, 1988, 6 (2): 223-229.

[20] Ehiasarian A P, New R, Münz W D, et al. Influence of high power densities on the composition of pulsed magnetron plasmas[J]. Vacuum, 2002, 65(2): 147-154.

[21] Alami J, Sarakinos K, Mark G, et al. On the deposition rate in a high power pulsed magnetron sputtering discharge[J]. Appl Phys Lett, 2006, 89(15): 154 104-3.

[22] Kouznetzov V. Method and apparatus for magnetically enhanced sputtering[P]. US Patent, 2001, US 6296742 B1.

[23] Sproul W D, Christie D J, Carter D C, et al. Pulsed plasma for sputtering applications[J]. Surf Eng, 2004, 20(3):174-180.

[24] Christie D J, Tomasel F, Sproul W D, et al. Power supply with arc handling for high peak power magnetron sputtering [J]. J Vac Sci Technol, A, Vac Surf Films, 2004, 22(4): 1 415-1 419.

[25] Alami J, Gudmundsson J T, Bohlmark J, et al. Plasma dynamics in a highly ionized pulsed magnetron discharge[J]. Plasma Sources Sci Technol, 2005, 14(3): 525-531.

[26] Anders A, Andersson J, Ehiasarian A. High power impulse magnetron sputtering: current-voltage-time characteristics indicate the onset of sustained self-sputtering[J]. J Appl Phys, 2007, 102(11): 113 303-11.

[27] Yukimura K, Mieda R, Azuma K, et al. Voltage-current characteristics of a high-power pulsed sputtering (HPPS) glow discharge and plasma density estimation[J]. Nucl Instrum Methods Phys Res B, 2009, 267(8/9): 1 692-1 695.

[28] Benzeggouta D, Hugon M C, Bretagne J, et al. Study of a HPPMS discharge in Ar/O_2 mixture: I. Discharge characteristics with Ru cathode[J]. Plasma Sources Sci Technol, 2009, 18(4): 045 025-9.

[29] Nakano T, Hirukawa N, Saeki S, et al. Effects of target voltage during pulse-off period in pulsed magnetron sputtering on afterglow plasma and deposited film structure[J]. Vacuum, 2013, 87: 109-113.

[30] Bugaev S P, Sochugov N S. Production of large-area coatings on glasses and plastics[J]. Surf Coat Technol, 2000, 131 (1-3): 474-480.

[31] Chistyakov R. Plasma source for semiconductor manufacturing industry e. g. plasma etching, has power supply to generate electric field ionizing volume of feed gas, and another supply generating another field super-ionizing initial plasma[P]. World Patent, 2004, WO 2004/095 497 A2.

[32] Bohlmark J, Lattemann M, Gudmundsson J T, et al. The ion energy distributions and ion flux composition from a high power impulse magnetron sputtering discharge[J]. Thin Solid Films, 2006, 515(4): 1 522-1 526.

[33] Konstantinidis S, Dauchot J P, Ganciu M, et al. Influence of pulse duration on the plasma characteristics in high-power pulsed magnetron discharges[J]. J Appl Phys, 2006, 99 (1): 013 307-5.

[34] Bohlmark J, Alami J, Christou C, et al. Ionization of sputtered metals in high power pulsed magnetron sputtering [J]. J Vac Sci Technol, A, Vac Surf Films, 2005, 23(1): 18-22.

[35] Erkens G, Cremer R, Hamoudi T, et al. Properties and performance of high aluminum containing (Ti, Al) N based supernitride coatings in innovative cutting applications[J]. Surf Coat Technol, 2004, 177-178: 727-734.

[36] Lin J, Moore J J, Sproul W D, et al. Ion energy and mass distributions of the plasma during modulated pulse power magnetron sputtering[J]. Surf Coat Technol, 2009, 203 (24): 3 676-3 685.

[37] Sch önjahn C, Ehiasarian A P, Lewis D B, et al. Optimization of in situ substrate surface treatment in a cathodic arc plasma: a study by TEM and plasma diagnostics [J]. J Vac Sci Technol A, 2001, 19(4): 1 415-1 420.

[38] Ehiasariana A P, Wen J G, Petrov I. Interface microstructure engineering by high power impulse magnetron sputtering for the enhancement of adhesion[J]. J Appl Phys, 2007, 101 (5): 054 301-10.

[39] Gudmundsson J T. Ionization mechanism in the high power impulse magnetron sputtering (HiPIMS) discharge[J]. J Phys, 2008, 100: 082 013-4.

[40] Bohlmark J, Gudmundsson J T, Alami J, et al. Spatial

electron density distribution in a high-power pulsed magnetron discharge[J]. IEEE Trans Plasma Sci, 2005, 33(2): 346-347.

[41] Stranak V, Herrendorf A P, Drache S, et al. Plasma diagnostics of low pressure high power impulse magnetron sputtering assisted by electron cyclotron wave resonance plasma[J]. J Appl Phys, 2012, 112(9): 093 305-9.

[42] Druyvesteyn M J. The low arc volt[J]. Z Phys, 1930, 64(11/12): 781-798.

[43] Lieberman M A, Lichtenberg A J. Principles of Plasma Discharges and Materials Processing[M]. 2nd ed, Wiley, New York. 2005:191.

[44] Hecimovic A, Arcos T de los, Schulz-von der Gathen V, et al. Temporal evolution of the radial plasma emissivity profile in HIPIMS plasma discharges[J]. Plasma Sources Sci Technol, 2012, 21(3): 035 017-9.

[45] Aiempanakit M, Aijaz A, Lundin D, et al. Understanding the discharge current behavior in reactive high power impulse magnetron sputtering of oxides[J]. J Appl Phys, 2013, 113(13): 133 302-8.

[46] Hecimovic A, Ehiasarian A P. Time evolution of ion energies in HIPIMS of chromium plasma discharge[J]. J Phys D: Appl Phys, 2009, 42(13): 135 209-9.

[47] Lundin D, Stahl M, Kersten H, et al. Energy flux measurements in high power impulse magnetron sputtering[J]. J Phys D: Appl Phys, 2009, 42(18): 185 202-7.

[48] Rohde D, Berndt J, Deutsch H, et al. Investigations on the energy influx at plasma processes by means of a simple thermal probe[J]. Thin Solid Films, 2000, 377-378: 585-591.

[49] Alami J, Persson P O Å, Music D, et al. Ion-assisted physical vapor deposition for enhanced film properties on nonflat surfaces[J]. J Vac Sci Technol A, 2005, 23(2): 278-280.

[50] Bobzin K, Bagcivan N, Immich P, et al. Mechanical properties and oxidation behaviour of (Al,Cr)N and (Al,Cr,Si)N coatings for cutting tools deposited by HPPMS[J]. Thin Solid Films, 2008, 517(3): 1 251-1 256.

[51] Sproul W D, Christie D J, Carter D C, et al. Pulsed plasmas foil sputtering applications[J]. Surf Eng, 2004, 20(3): 174-176.

[52] Vl ek J, Pajdarová A D, Musil J. Pulsed dc magnetron discharges and their utilization in plasma surface engineering[J]. Contrib Plasma Phys, 2004, 44(5/6): 426-436.

[53] Christie D J. Target material pathways model for high power pulsed magnetron sputtering[J]. J Vac Sci Technol, A, Vac Surf Films, 2005, 23(2): 330-335.

[54] Konstantinidis S, Dauchot J P, Ganciu M, et al. Influence of pulse duration on the plasma characteristics in high-power pulsed magnetron discharges[J]. J Appl Phys, 2006, 99(1): 013 307-5.

[55] Alami J, Eklund P, Andersson J M, et al. Phase tailoring of Ta thin films by highly ionized pulsed magnetron sputtering[J]. Thin Solid Films, 2007, 515(7/8): 3 434-3 438.

[56] Hosokawa N, Tsukada T, Kitahara H. Preparation and properties of carbon-films with magnetron sputtering[R]. Proceedings of the 8th International Vacuum Congress, 1980, Cannes, France, 1: 115-116.

[57] Bugaev S P, Koval N N, Sochugov N S, et al. Investigation of a high-current pulsed magnetron discharge initiated in the low-pressure diffuse arc plasma[C]//Proceedings of the 17th International Symposium on Discharges and Electrical Insulation in Vacuum, 1996, Berkeley, CA, USA, 1/2: 1 074-1 076.

[58] Konstantinidis S, Dauchot J P, Ganciu M, et al. Transport of ionized metal atoms in high-power pulsed magnetron discharges assisted by inductively coupled plasma[J]. Appl Phys Lett, 2006, 88(2): 021 501-3.

[59] Bohlmark J, Östbye M, Lattemann M, et al. Guiding the deposition flux in an ionized magnetron discharge[J]. Thin Solid Films, 2006, 515(4): 1 928-1 931.

[60] Alami J, Sarakinos K, Uslu F, et al. On the relationship between the peak target current and the morphology of chromium nitride thin films deposited by reactive high power pulsed magnetron sputtering[J]. J Phys D: Appl Phys, 2009, 42(1): 015 304-7.

[61] Bagcivan N, Bobzin K, Theiß S. $(Cr_{1-x}Al_x)N$: a comparison of direct current, middle frequency pulsed and high power pulsed magnetron sputtering for injection molding components[J]. Thin Solid Films, 2013, 528: 180-186.

[62] Partridge J G, Mayes E L H, McDougall N L, et al. Characterization and device applications of ZnO films deposited by high power impulse magnetron sputtering (HiPIMS)[J]. J Phys D: Appl Phys, 2013, 46(16): 165 105-5.